

# The temperature calibration of a parallel plate rheometer and evaluation of the thermal lags during polymer solidification

W. Zhang, J.A. Martins\*

*IPC, Departamento de Engenharia de Polímeros, Universidade do Minho, Campus de Azurém, 4800-058 Guimarães, Portugal*

Received 20 June 2003; received in revised form 27 October 2003; accepted 28 October 2003

## Abstract

Parallel plate rheometers are often employed for analysing the effect of small amplitude oscillations, with different frequencies, on the crystallization of polymers. Practical problems associated to this application are analysed and discussed with emphasis on those involved with the temperature measurements and the true sample temperature evaluation. A temperature calibration method of these devices, for nominally isothermal and cooling experiments, is tested through simultaneous measurements of the sample temperature performed with an additional thermocouple. The magnitude and errors of the isothermal correction are evaluated and their effect on the recorded experimental data is also discussed. For isothermal and nonisothermal experiments, the additional thermal effects ascribed to the sample thermal resistance and to the heat of crystallization released during the solidification are also evaluated. The effect of these corrections over DSC and rheometer results is analysed and discussed.

© 2003 Elsevier B.V. All rights reserved.

*Keywords:* Shear; Crystallization; Isothermal; Nonisothermal; Thermal lags

## 1. Introduction

Parallel plate rheometers, and modified devices with a similar working principle, have been widely used for studying the effect of shear flow on the crystallization of polymers, mainly for isothermal conditions [1–3]. The variation of modulus and viscosity of polymer melts with time may be used to describe changes of their physical state, such as those occurring during crystallization processes, since its earlier stages [4], where the crystallization may be viewed as a physical gelation process. As for the effect of shear on crystallization kinetics, it is known that the shear rate increases the nucleation density and the crystallization kinetics.

Known the importance that the crystallization temperature has on the determination of the nucleation density and growth rate, its precise definition is crucial for evaluating the effective role played by the shear rate on the crystallization kinetics, and for comparing small angle oscillatory shear with DSC experiments. That precision is limited by the accuracy of the thermocouple used, by the device

and sample thermal resistances, and it is also dependent on the heat of crystallization released during the phase change.

In the present work, the errors associated with the temperature measurements during the isothermal and, especially, nonisothermal crystallization of a sheared melt in a parallel plate rheometer are evaluated and checked against experimental data. Calibration methods currently used for the temperature calibration of other thermal analysis devices are applied for calibrating the temperature scale of a rheometer. The different thermal lags are then evaluated separately, their effect on the overall crystallization kinetics is analysed, and the true sample temperature during the crystallization process is estimated. The validity of these procedures is assessed through complementary temperature measurements, in real time, of the sample under study by comparing the measured and the estimated sample's temperatures. Also, for justifying the need for correcting the nominal temperature data, the rheometer results for constant crystallization temperatures are compared, before and after the temperature corrections, with differential scanning calorimetry results following a similar crystallization temperature program. Some published literature results are also used for illustrating the importance in estimating the true sample temperature.

\* Corresponding author. Tel.: +351-253510325; fax: +351-253510339.  
*E-mail address:* [jamartins@dep.uminho.pt](mailto:jamartins@dep.uminho.pt) (J.A. Martins).

It is often assumed that the temperature recorded by the rheometer oven's thermocouple is near to the real sample temperature, and that this approximation is within the errors ascribed by the equipment manufacturers, which is usually small, around  $\pm 0.2^\circ\text{C}$ . The error is in fact larger than the specified manufacturer's value, and the temperature recorded, both for isothermal and scanning rate conditions, must be corrected for compensating the isothermal and rate dependent thermal lags. Additional temperature corrections allow the estimation of the sample temperature by accounting for the different material thermal conductivity and heat of crystallization released during the solidification.

Procedures and substances for calibrating the temperature of thermal analysis devices, such as differential scanning calorimeters or differential thermal analysers, are described with detail in literature and their routine application is a standard practice. On the contrary, some commercial software of rheometers does not allow inputting temperature calibration values, and in just a few works the temperature calibration of these devices is explicitly mentioned, together with the calibration substances. Among them is the work of Acierno et al. [5], where the temperature scale of a rheometer is calibrated with three standards (naphthalene, benzoic acid and indium) and, apparently, only for heating and eventually for isothermal experiments. The work did not point out the magnitude of the different thermal corrections and the temperature errors involved in the measurements.

In this work, the same high purity metal standards, used for calibrating other thermal analysis devices, are used for calibrating the temperature scale of a rheometer. Ideally, three standards should be used, but, since the working temperature range is relatively narrow, we have selected only indium (In) and tin (Sn). When the heating calibration is performed with two standards, two temperature corrections are automatically performed: the isothermal correction, at the melting temperature of the standards, and a rate-dependent thermal lag, which increases with the heating rate. The true sample temperature of a high thermally conductive material ( $T_t^+$ ) may be evaluated, for a particular heating rate, by a linear relation with the measured temperature ( $T_m$ ).

The isothermal correction, evaluated from experiments at several heating rates by extrapolation of the measured onset values for the melting of the standards to zero scanning rate,  $T_{m,0}$ , is  $\Delta T_0 = T_{m,0} - T_{\text{exp},0}$ , where  $T_{\text{exp},0}$  is the expected (true) temperature. The variation of this correction in the working temperature range may be assumed to be linear,  $\Delta T_0 = a_0 T_m + b_0$ , where the constants  $a_0$  and  $b_0$  may be evaluated from the extrapolated standards' onset values to zero scanning and the corresponding isothermal corrections at their melting temperatures.

This isothermal correction should be the same for all experiments, while the correction resulting from the rate thermal lag should be symmetrical for heating and cooling scans. It was shown in a previous work [6] that, if the scanning rate thermal lags are symmetrical for heating and cooling experiments, the calibration on cooling may be performed

from the calibration on heating according to

$$T_t^- = (2 - a^+)T_m - 2\Delta T_0 + b^+, \quad (1)$$

where  $T_t^-$  is the true sample temperature for a cooling experiment. The error with which this calibration was performed for differential scanning calorimeters was evaluated with liquid crystalline transitions of high-purity liquid crystals. The same procedures were here applied for the temperature calibration of a parallel plate rheometer: the calibration on heating was performed from heating experiments at different heating rates that were further used to perform the isothermal correction and the calibration on cooling.

By evaluating the thermal lag due to the sample's thermal resistance and the heat of crystallization released during the phase change, the average true sample temperature may be estimated from the following heat balance: the sensible heat flux received by the sample equals the difference between the heat flux released within the sample due to the ongoing crystallization process and the instrument-sensed net heat loss from the sample to the corresponding temperature sensor [7,8] i.e.,

$$m\bar{c}_p \frac{dT_t}{dt} = m|\Delta h_c| \frac{dX}{dt} - \frac{1}{R_s}(T_t - T_m), \quad (2)$$

where  $m$  is the sample mass,  $\bar{c}_p$  the specific heat capacity,  $dT_t/dt$  the rate of the true sample temperature variation,  $R_s$  the sample's thermal resistance and  $T_t$  and  $T_m$  are the true sample temperature and the temperature measured by the temperature sensor, respectively. The heat flux released within the sample is  $m|\Delta h_c|dX/dt$ , where  $\Delta h_c$  is the heat of crystallization and  $X$  the mass fraction transformed (or relative crystallinity) at time  $t$ . The sample's thermal resistance  $R_s$  is a function of the sample's dimensions, thickness ( $b$ ) and area ( $A$ ), and the material thermal conductivity ( $k$ )— $R_s = b/Ak$ , where, for the rheometer samples, the sample's thickness is the measured gap size. The average true sample temperature may then be evaluated by solving numerically Eq. (2). Since the temperature profile across the sample's thickness was not estimated in this work, it is assumed that the temperature estimated from Eq. (2) is the average temperature of the sample.

## 2. Experimental

### 2.1. Samples

The temperature calibration was performed with high purity metals supplied by Goodfellow Limited Company, Cambridge, England. The purity and melting points of the metals used were: indium 99.99999% and  $156.6^\circ\text{C}$ ; tin 99.9999% and  $231.9^\circ\text{C}$ ; lead 99.999% and  $327.5^\circ\text{C}$ , respectively.

For the isothermal crystallization experiments, a high-density polyethylene supplied by Borialis, Portugal, grade BS2581P, with a melt flow index of  $0.3\text{ g}/10\text{ min}$  (evaluated

according to the norm ISO 1133) and density  $958 \text{ Kg m}^{-3}$ , was selected. Its thermodynamic melting temperature, evaluated by a Hoffman and Weeks plot, was  $145^\circ\text{C}$  and the average heat of fusion, for the samples crystallized in the DSC at temperatures ranging from  $118$  to  $128^\circ\text{C}$ , was  $192 \text{ J g}^{-1}$  with a standard deviation of  $6.9 \text{ J g}^{-1}$ . Constant values were used for the material's thermal conductivity and specific heat capacity,  $0.42 \text{ W K}^{-1} \text{ m}^{-1}$  and  $1.6 \text{ J K}^{-1} \text{ Kg}^{-1}$ , respectively.

## 2.2. DSC experiments

A Perkin-Elmer DSC-7 (Norwalk, CT) running in standard mode was used. The temperature of the cold block was kept at  $5^\circ\text{C}$  and the nitrogen purge-gas flow rate was  $20 \text{ cm}^3/\text{min}$ . Previous temperature and enthalpic calibrations were carried out according to the standard procedures described on the DSC7 Perkin-Elmer Manual. For the isothermal experiments, the temperature calibration was performed at  $0.1^\circ\text{C}/\text{min}$  and checked before and after a set of experiments. Deviations of  $\pm 0.2^\circ\text{C}$  for the measured onset were obtained, and it will be assumed that this is the error for the crystallization experiments carried out in these conditions.

The samples for DSC experiments, with around  $10.522 \text{ mg}$ , were prepared by controlling the thickness and area for further evaluating their thermal resistance. Average values of the sample's thickness and diameter were  $0.458 \text{ mm}$  and  $5.062 \text{ mm}$ , respectively. For the isothermal crystallization experiments, the sample was held at  $180^\circ\text{C}$  for  $1 \text{ min}$ , then cooled down to the desired crystallization temperature at a controlled cooling rate of  $-60^\circ\text{C}/\text{min}$ . For elimination of the transient originated by the jump from the initial temperature to the crystallization temperature, a blank experiment was performed in a temperature range above the melting temperature of the polymer. Non-isothermal experiments at several scanning rates, starting from the melt, were also performed. The nominal temperature recorded for these experiments was corrected with Eq. (1), for correcting the isothermal thermal lag and the thermal lag due to the cooling rate, and (2), for correcting the additional thermal lags resulting from the sample's thermal resistance and release of the heat of crystallization.

## 2.3. Rheometer experiments

A Rheologica StressTech rheometer (Rheologica Instruments AB, Sweden), with parallel plate geometry ( $25 \text{ mm}$  diameter) was used for studying the effect of shear on the polymer crystallization kinetics and for testing the temperature corrections procedures. The experiments over indium and tin were performed at a constant stress of  $12 \text{ kPa}$ , and oscillation frequency of  $1 \text{ Hz}$ , at various heating rates. The isothermal crystallization experiments were performed following a temperature program similar to the one used for the

DSC experiments, with the exceptions of cooling rate and starting temperature, where a cooling rate of  $-20^\circ\text{C}/\text{min}$  and a starting temperature of  $170^\circ\text{C}$  were used instead. The dwell time at the crystallization temperature was certified to be long enough to completely record the solidification process, as detected by the stabilization of the material's storage modulus after a steep increase. The nonisothermal crystallization experiments were performed at several cooling rates, following a temperature program similar to the one followed in the corresponding DSC experiments.

Both, isothermal and nonisothermal, experiments were performed at oscillation frequencies of  $0.1$ ,  $1$  and  $10 \text{ Hz}$ , with a constant stress of  $1 \text{ kPa}$ , since it was found, by a series of stress sweep experiments, that this stress ensures linear viscoelastic behaviour in the temperature range of interest. The values of the strain over the samples were recorded during the experiment ( $3\%$  at the beginning and around  $0.1\%$  at the end), together with the values of the gap size. Both values were decreasing during the experiment thus ensuring that the sample is within the linear viscoelastic region and that, as in the work of Boutahar et al. [9], the longitudinal efforts induced by the dimensional variation of the sample are eliminated.

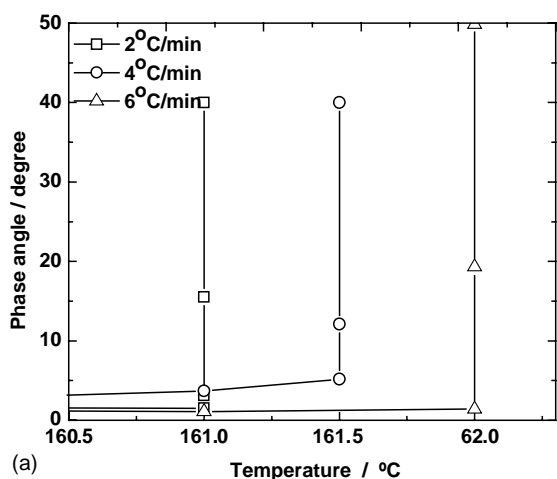
The rheometer samples were prepared by a previous melting of the polymer pellets in a hot-press machine at  $190^\circ\text{C}$ . A plate with around  $2 \text{ mm}$  of thickness was obtained, from which circular disks with  $25 \text{ mm}$  of diameter were cut for use in the rheometer.

Simultaneously with the rheological experiments, the sample temperature was measured with a K-type thermocouple (HKMTSS-010G-6 from OMEGA) and further recorded. The response time of the thermocouple is lower than  $0.3 \text{ s}$  and its temperature accuracy, evaluated after several sets of measurements in a controlled temperature bath, was  $\pm 0.5^\circ\text{C}$ .

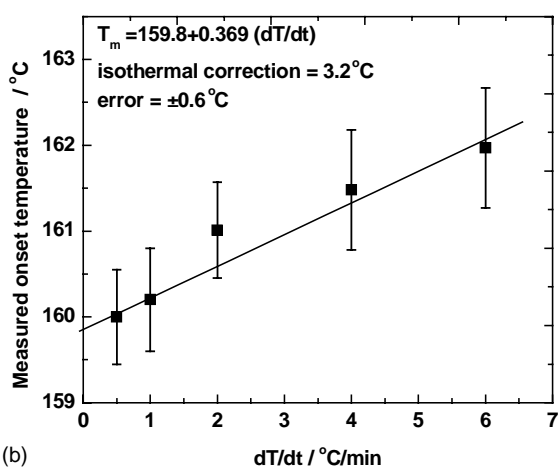
## 3. Results and discussion

### 3.1. Temperature calibration

The accuracy of the temperature recorded by the temperature sensor of the parallel plate rheometer was assessed with two metal standards, indium and tin. They were heated up to a temperature higher than their melting temperature, and further pressed to produce a film with around  $0.1 \text{ mm}$  of thickness and a diameter equal to that of the upper plate ( $25 \text{ mm}$ ). The scans at several heating rates (from  $0.1$  to  $6^\circ\text{C}/\text{min}$ ) were then performed, starting at temperature such that, the difference between the starting and the expected melting temperatures, divided by the heating rate, was higher than  $5 \text{ min}$ . With this procedure, a well defined "baseline" is ensured before the detection of the transition. A dwell time of  $10 \text{ min}$  was allowed for all experiments to guarantee an adequate temperature stabilisation at the start. The onset of melting was assigned to the sudden increase of the phase



(a)

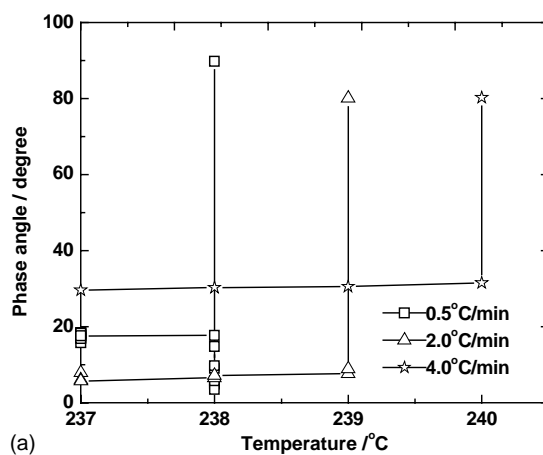


(b)

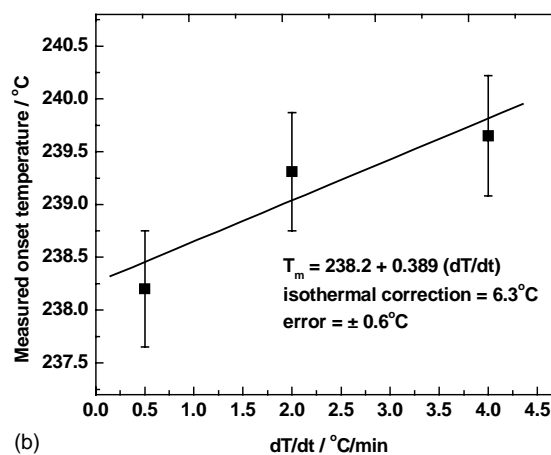
Fig. 1. Heating rate dependence for the melting onset of indium. (a) Detection of the onset of melting in a parallel plate rheometer by the sudden increase of the phase angle at the frequency of 1 Hz and scanning rates of 2, 4 and 6 °C/min, and (b) evaluation of the isothermal correction at zero scanning rate for the indium melting temperature ( $\Delta T_0 = 3.2 \pm 0.6^\circ\text{C}$ ).

angle, coincident with the sudden decrease of the viscosity. For avoiding contamination of the oven with the metal, these experiments were suddenly stopped just after the detection of the onset of melting. For evaluating the measurement errors, each melting experiment, at the same heating rate, was repeated at least three times.

The results obtained for the variation of the indium phase angle with the temperature, at several heating rates, are in Fig. 1a. Fig. 1b shows the corresponding change of the onset of melting as a function of the heating rate and the associated measurement errors around the mean. These results show that, on heating, the temperature recorded by the rheometer thermocouple is higher than the sample (metal) temperature. As expected, the difference increases with the heating rate. Since dynamic experiments, of the type carried out in Fig. 1a, are unusual in rheometry, it is more relevant evaluating the temperature errors for isothermal (or nearly isothermal) conditions. The isothermal correction at the indium melting temperature ( $156.6^\circ\text{C}$ ), evaluated



(a)



(b)

Fig. 2. Heating rate dependence for the melting onset of tin. (a) Detection of the onset of melting in a parallel plate rheometer by the sudden increase of the phase angle at the frequency of 1 Hz and scanning rates of 0.5, 2 and 4 °C/min, and (b) evaluation of the isothermal correction at zero scanning rate for the tin melting temperature ( $\Delta T_0 = 6.3 \pm 0.6^\circ\text{C}$ ).

by extrapolating the line fitting the data of Fig. 1b to zero scanning rate, is  $3.2 \pm 0.6^\circ\text{C}$ . Furthermore, this isothermal correction should be the same for heating and cooling experiments, that is, it should be independent of the way used to reach the isothermal temperature, from higher (cooling) or from lower (heating) temperatures.

Similar results were obtained for tin and they are in Fig. 2a and b. The main difference here is the magnitude of the isothermal correction. The value obtained for this correction at the melting temperature of tin ( $231.9^\circ\text{C}$ ) is  $6.3 \pm 0.6^\circ\text{C}$ . The variation of the isothermal correction in the temperature range between  $156.6$  and  $231.9^\circ\text{C}$  may be attributed to the non-linear variation of the thermocouple electromotive force in the same temperature range. As a reasonable approximation, and as indicated in the introduction, it will be assumed a linear variation of  $\Delta T_0$  with the measured temperature in the temperature range of work.

The results of Figs. 1 and 2 allow calibrating the temperature scale of the rheometer at any controlled heating rate and also for nominally isothermal experiments. However, for

this last case, the isothermal temperature must be reached starting from lower temperatures. Actually, the results that will be shown below, will demonstrate that the isothermal correction, for the device used in this work, is (unexpectedly) dependent on temperature program path towards the isothermal temperature. This has clear implications on the evaluation of the sign of this correction, and hence on the evaluation of the temperature calibration on cooling.

### 3.2. True sample temperature for nominally isothermal scans

For checking the validity of the temperature calibration procedures, the sample temperature was recorded with an external thermocouple inserted into the sample. During these experiments, it was ensured that the presence of the thermocouple did not disturb the sample thermal environment and the measured modulus values from which the crystallization kinetics was evaluated. Fig. 3a and b shows the results obtained for the isothermal experiments. Also here, before the residence time of 2 min at the starting nominally isothermal temperature (170 °C), which was reached by heating

the sample from the room temperature with the maximum heating rate allowed by the device, the temperature was kept stable during 10 min for allowing the sample temperature equilibration and to guarantee isothermal conditions at the start of the experiment.

The inset in Fig. 3a shows that, at the starting temperature, the true sample (measured) temperature is  $166.7 \pm 0.6$  °C, which is  $3.3 \pm 0.6$  °C below the program temperature, in good agreement with the predicted isothermal correction for 170 °C,  $3.8 \pm 0.6$  °C. The next step is the cooling down to the crystallization temperature, and it is observed that the sample temperature is delayed with respect to the program temperature, the sample being now at a higher temperature than that recorded by the rheometer temperature sensor. During the isothermal crystallization process, the delay is maintained and the sample temperature stabilizes at  $129.3 \pm 0.6$  °C.

At this stage, it is important a careful analysis of the results obtained, in light of the definition of isothermal correction, which should be independent on the approach towards the nominally isothermal temperature. The predicted correction for 127 °C is  $2.0 \pm 0.6$  °C, which would mean that the real sample temperature should then be  $125 \pm 0.6$  °C. What is observed from the temperature recorded by the sample thermocouple is that, for the instrument used in this work, the sign of the isothermal correction is positive when the nominally isothermal temperature is reached starting from lower temperatures (the sample is at a lower temperature than the one indicated by the rheometer temperature sensor, see inset of Fig. 3a). The opposite occurs when the nominally isothermal temperature is reached starting from higher temperatures (see Fig. 3b), where the isothermal correction is  $-2.3 \pm 0.6$  °C, in agreement with the predicted value of  $-2.0 \pm 0.6$  °C. This strange behaviour may be ascribed to the rheometer oven's device conception, and it is certainly a result of the high thermal inertia of the system.

The accounting of this observation is important for evaluating errors, for example, in frequency sweep measurements where deviations equal to twice the isothermal correction may exist in consecutive experiments depending on the approach to the isothermal temperature. These deviations may be confirmed with the flow curves of Fig. 4, where it is shown the variation of the storage modulus with the oscillation frequency for the nominal temperature of 170 °C, when this temperature is reached starting from 30 °C—curve (a), and from 220 °C—curve (b). Even though these experiments were executed at the same nominal temperature, the temperature difference of the sample between the results of curves (a) and (b) is around 7 °C. For nominally higher isothermal temperatures, this difference is accentuated.

The results obtained for the isothermal crystallization recorded with the rheometer are in Table 1. The table shows, for several nominal crystallization temperatures, the predicted isothermal crystallization temperature (assuming the symmetry of the isothermal correction mentioned previously) and the temperature measured with the external thermocouple for different oscillation frequencies. The

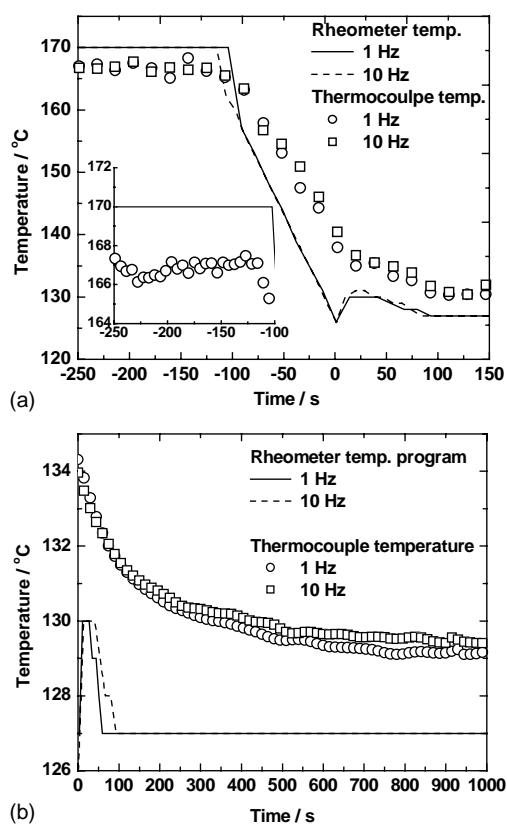


Fig. 3. Variation of the measured sample temperature, recorded with an external thermocouple, and the rheometer program temperature with time at the indicated frequencies during the isothermal crystallization at the nominal temperature of 127 °C. The symbols show the measured temperature, (○) 1 Hz and (□) 10 Hz, and the lines show the rheometer program temperature. (a) Transition to the crystallization temperature and (b) residence time at the crystallization temperature.



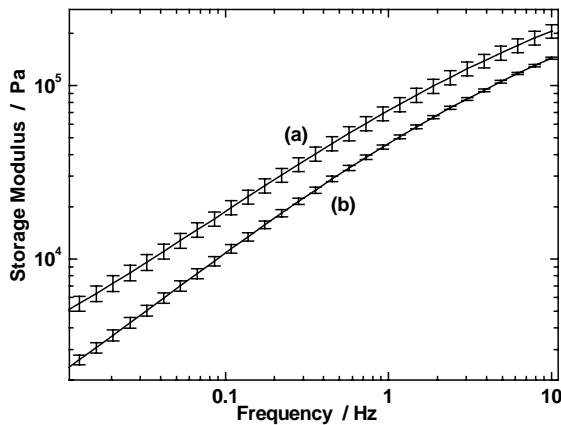


Fig. 4. Variation of the storage modulus with the oscillation frequency at nominal temperature of 170 °C. (a) Nominal temperature reached starting from 30 °C and (b) nominal temperature reached starting from 220 °C. The curves shown are the average values of three consecutive experiments carried out with a constant stress of 1 kPa and gap size of 0.6 mm. The error bars are the standard error of the mean.

agreement between these results is within experimental error limits, with the exception of the value obtained for 128 °C and oscillation frequency of 10 Hz. For this particular case, the sample thickness is approximately equal to the thermocouple diameter (0.25 mm), being this the most probable explanation for the deviation observed.

The evaluation of the degree of conversion to the solid phase for the rheometer data was made through the variation with time of the storage modulus using an equation proposed by Khanna [10],

$$X(t, T) = \frac{G'(t, T) - G'(0, T_m^0)}{G'(t_s, T_s) - G'(0, T_m^0)}, \quad (3)$$

and another one proposed by Boutahar et al. [9] which, according to the authors, allows an accurate evaluation for the degree of conversion to the solid phase up to 0.84 of the conversion degree,

$$X(t, T) = \left[ \frac{G'(t, T) - G'(0, T_m^0)}{G'(t_s, T_s) - G'(0, T_m^0)} \right]^{1/3} \quad (4)$$

where  $G'(0, T_m^0)$ ,  $G'(t, T)$  and  $G'(t_s, T_s)$  are the storage modulus at time zero (or at a temperature greater than the ther-

modynamic melting temperature,  $T_m^0$ ), at time  $t$  (or at the current crystallization temperature) and at time  $t_s$  (or a temperature  $T_s$ ) where the liquid is fully converted to the solid phase, respectively. The dependent variables, time and temperature, are used for isothermal and nonisothermal scans, respectively. The purpose of this exercise is the comparison of the results obtained with the above two equations.

However, the extension of the above two equations to nonisothermal experiments may be questioned since the recorded changes of the storage modulus may be ascribed both to relaxation mechanisms and to the development of the solid phase. The magnitude of the change due to this last process is much larger than the one originated by the relaxation mechanisms. For a cooling rate of  $-1$  °C/min, the storage modulus changes between 15 and 30 kPa in a temperature window between 120 and 170 °C. The crystallization develops in a temperature interval of 10 °C (between 120 and 110 °C) and a stable value of the modulus is reached for the solid state (2 GPa). The evaluation of the modulus variation due to the relaxation mechanisms is important for a precise evaluation of the nonisothermal crystallization recorded with a parallel plate rheometer. However, from the above discussion, it is expected a negligible effect in face of the large value of the modulus measured for the solid state and the relatively narrow temperature interval where the crystallization occurs.

The validity of Eq. (3) for evaluating the degree of conversion to the solid phase from low frequency rheological data was questioned by Allig et al. [11]. In this work, the Avrami's equation is included in series, parallel and other models to fit the experimental data. Since the assessment of validity was based on the quality of the fitting to the experimental results, the procedure used by these authors is questionable because the Avrami's equation requires a homogeneous distribution of nuclei at all times during the crystallization process. This does not occur in the crystallization recorded with a parallel plate rheometer, the distribution of nuclei being different at the centre and extremity of the sample.

The results obtained for  $T_c = 121 + 1.7 \pm 0.6$  °C =  $122.7 \pm 0.6$  °C are in Fig. 5. The figure shows that the evaluation of the degree of conversion to the solid phase for the rheometer data results in a slower crystallization kinetics in

Table 1  
Information of isothermal crystallization in the rheometer at the temperatures and frequencies indicated

$T_m$ (°C)	$T_i^a$ (°C)	$\omega = 0.1$ Hz		$\omega = 1$ Hz		$\omega = 10$ Hz	
		gap (mm)	$T_{th}^b$ (°C)	gap (mm)	$T_{th}^b$ (°C)	gap (mm)	$T_{th}^b$ (°C)
118	119.6	0.791	119.2	0.638	119.1	0.549	119.1
121	122.7	0.722	122.1	0.535	122.6	0.409	122.3
124	125.9	0.810	125.3	0.630	124.7	0.487	125.0
127	129.0	0.427	128.3	0.458	129.2	0.444	129.5
128	130.0	0.386	129.5	0.406	129.4	0.262	128.4
129	131.1	0.438	130.7	0.427	130.4	0.438	130.1

<sup>a</sup> Temperature corrected after the isothermal correction (error  $\pm 0.6$  °C).

<sup>b</sup> Temperature measured by a thermocouple inserted into the sample (error  $\pm 0.5$  °C).

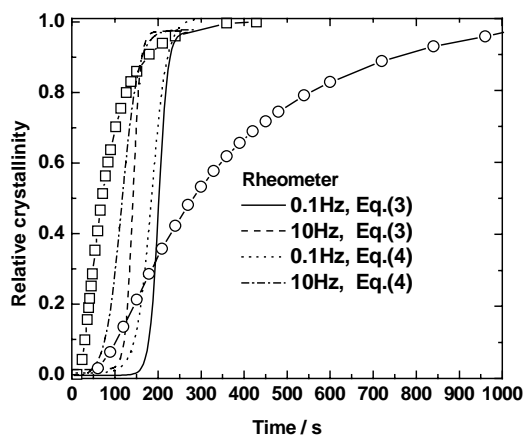


Fig. 5. Comparison of the crystallization kinetics of HDPE in a DSC at 121 °C (—□—) and 123 °C (—○—) with that recorded with a parallel plate rheometer at the temperature  $T_c + \Delta T_0 = 122.7$  °C and at the frequencies indicated.

comparison with the DSC results at 121 °C. When Eq. (4) is used for evaluating the degree of conversion to the solid phase, the crystallization curves are shifted to lower crystallization times. Since it is known that shear deformations accelerate the nucleation density and the crystallization kinetics, if we had assumed no need for the isothermal correction, the results obtained were then unacceptable (note that the crystallization kinetics in the rheometer, as measured by the half of crystallization time, would then be slower than the crystallization in quiescent conditions at the same crystallization temperature). Results similar to those shown in Fig. 5 may be found in published works, for example in [3] and [9].

To our knowledge, in the works published so far for studying the effect of shear on the isothermal and non-isothermal crystallization with parallel plate rheometers, the effects of additional thermal lags on the average true sample temperature definition were not analysed. It has been implicitly assumed that the temperature accuracy of the shearing device is good enough, and that the effects of the thermal lags are negligible. This is a questionable assumption since the sample's thermal resistance in a parallel plate (or cone and plate) rheometer is much larger than that of the samples used, for example, in Linkam hot stages, thus generating much higher thermal lags.

Therefore, for evaluating the true sample temperature during the phase change, the additional effects resulting from the sample's thermal resistance and release of the heat of crystallization must also be considered. For this evaluation, the value of the measured sample gap size during the crystallization process was used, together with the specific sample information ( $m \approx 4 \times 10^{-4}$  Kg,  $\Delta h = 192$  J/g,  $c_p = 1.6$  J K $^{-1}$  Kg $^{-1}$  and  $R_s \approx 0.9$  K/W), to evaluate from Eq. (2) the sample temperature increase during the crystallization.

Fig. 6a and b show the results and its variation during the crystallization process, for the crystallization tem-

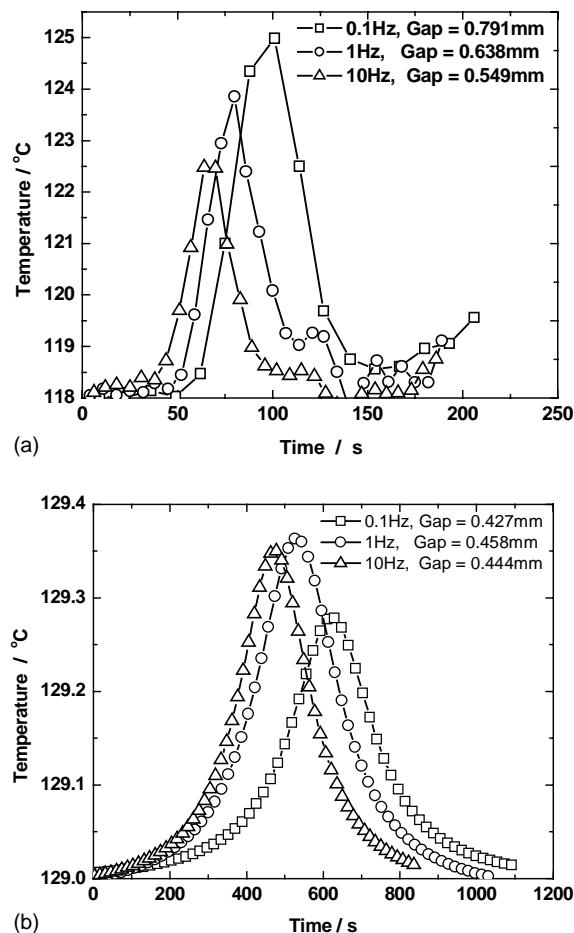


Fig. 6. Predicted temperature increase for the isothermal crystallizations in the rheometer at (a)  $119.6 \pm 0.6$  °C and (b)  $129 \pm 0.6$  °C. The nominal temperatures, without the isothermal correction, were 118 and 127 °C, respectively. The frequencies tested and sample's thickness are indicated in the figures.

peratures of  $119.6 \pm 0.6$  and  $129 \pm 0.6$  °C, respectively. The temperature increase is small, and almost meaningless, for high crystallization temperatures, but it is relevant for lower crystallization temperatures. The explanation is that the crystallization kinetics is faster and the heat of crystallization is released in a short time interval for lower crystallization temperatures. Therefore, the temperature increase certainly plays an important role on the definition of the average crystallization temperature and, consequently, on the overall crystallization kinetics. As in quiescent crystallization, Fig. 6a also clearly reveals that the temperature increase is smaller for thinner samples due to their lower mass and thermal resistance. For Fig. 6b, the gap sizes at different frequencies are almost identical, and for the oscillation frequencies used in this work, the temperature increase due to the sample's thermal resistance and the release of the heat of crystallization appears to be almost oscillation frequency independent. The temperature increase due to the viscous dissipation was evaluated following a methodology proposed by Ding et al. [12]

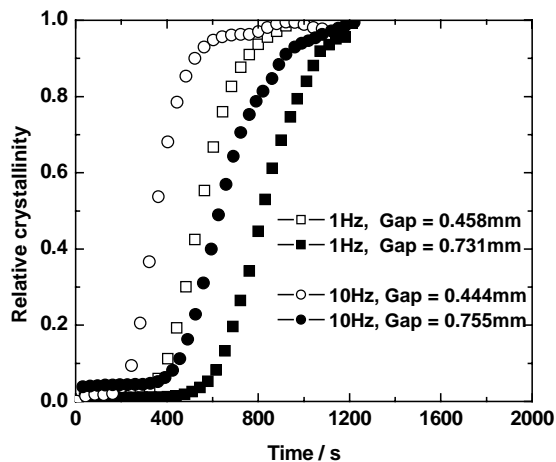


Fig. 7. Variation of the relative crystallinity with time for the isothermal crystallization of HDPE at  $T_c + \Delta T_0 = 129 \pm 0.6^\circ\text{C}$  and frequencies of 1 and 10 Hz, with the gap sizes indicated.

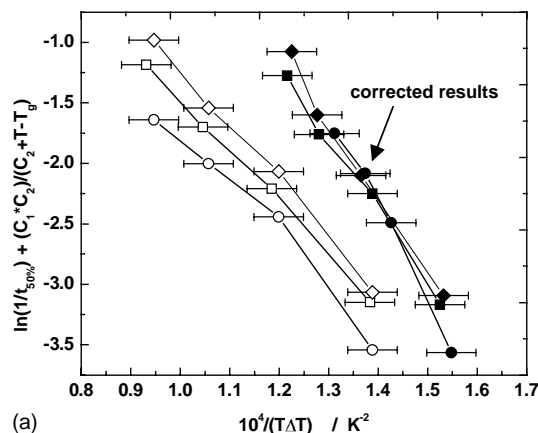
and the results obtained indicate that it was lower than  $0.01^\circ\text{C}$ .

The evaluation of the sample thickness (gap size) effect on the overall crystallization kinetics is of utmost importance for obtaining reproducible results. Fig. 7 shows the effect of the sample thickness on the overall crystallization kinetics: the isothermal crystallization rate (as evaluated for example by the value of the half of crystallization time) distinctly increases with the decrease of the gap size for the same oscillation frequency.

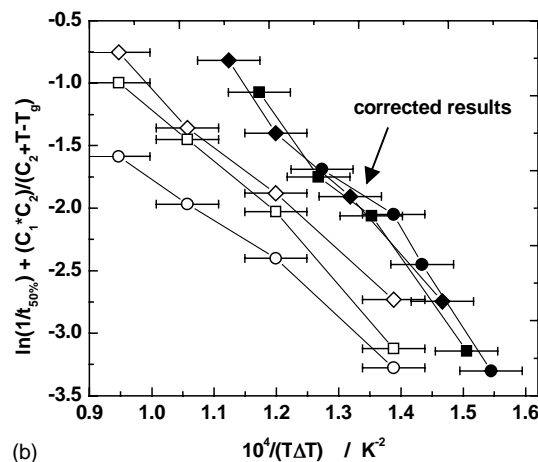
Since the data of Fig. 7 refer to the same crystallization temperature, it is expected that the differences shown are a consequence of the different sample thickness, effect that can be accounted for by evaluating the average true sample temperature. Since, even in nominally isothermal crystallization experiments, the sample temperature is changing, a time corresponding to the half of crystallization and the estimated true sample temperature at that time was used for analysing the results of Fig. 7.

It is assumed that, also for shear induced crystallization experiments, the temperature dependence of  $\ln(1/t_{50\%})$  is proportional to  $1/(T\Delta T)$ , where  $\Delta T$  is the supercooling. The assumption is based on a similar temperature dependence for the reciprocal of the half-crystallization time and the spherulite growth rate, where the diffusion term is assumed to have a WLF functionality  $[C_1 C_2 / (C_2 + T - T_g)]$ ;  $C_1$  and  $C_2$  are universal constants, equal to 25 and 30 K, respectively,  $T_g$  is the glass transition temperature of the polymer and  $T$  is the crystallization temperature. The nucleation term is dependent on the surface energies for nucleation and the elastic strain energy [13].

The results obtained after estimating the sample temperature at  $t_{50\%}$  are in Fig. 8a and b for the oscillation frequencies of 1 and 10 Hz, respectively. For these figures, all the results plotted with open symbols ( $\square$ ,  $\circ$ ,  $\diamond$ ) correspond to the nominal rheometer crystallization tempera-



(a)



(b)

Fig. 8. Variation of  $\ln(1/t_{50\%})$  with  $1/(T\Delta T)$  for the results of Fig. 7 and Table 1. (a) Oscillation frequency of 1 Hz and (b) oscillation frequency of 10 Hz. For both figures, the open symbols ( $\square$ ,  $\circ$ ,  $\diamond$ ) correspond to the nominal rheometer crystallization temperature. The results shown by ( $\square$ ) and ( $\diamond$ ) correspond to the same data (Table 1). For ( $\square$ ) the  $t_{50\%}$  was estimated with  $X(t)$  evaluated from Eq. (3), while for ( $\diamond$ ) the  $X(t)$  was evaluated from Eq. (4). For the results with thicker samples ( $\circ$ ) only Eq. (3) was used. All corresponding full symbols represent the true sample temperatures at the half of crystallization time.

ture. The results shown by ( $\square$ ) and ( $\diamond$ ) correspond to the same data (Table 1). The only difference between them is that for ( $\square$ ) the sample temperature at the half of crystallization time was estimated with  $X(t)$  evaluated from Eq. (3), while for ( $\diamond$ ) the  $X(t)$  was evaluated from Eq. (4). For the results with thicker samples ( $\circ$ ) only Eq. (3) was used. All the full symbols in Fig. 8a and b represent the corrected temperatures, that is, the temperature at the half of crystallization time corrected for the sample's thermal resistance and release of the heat of crystallization. The error bars show the errors related to the rheometer temperature measurement.

After the average true sample temperature evaluation, the deviation between the results obtained for samples with different thicknesses are within the experimental measurement errors ( $\bullet$ ,  $\blacksquare$ ). Also, the deviation between the results obtained for the same sample with Eqs. (3)



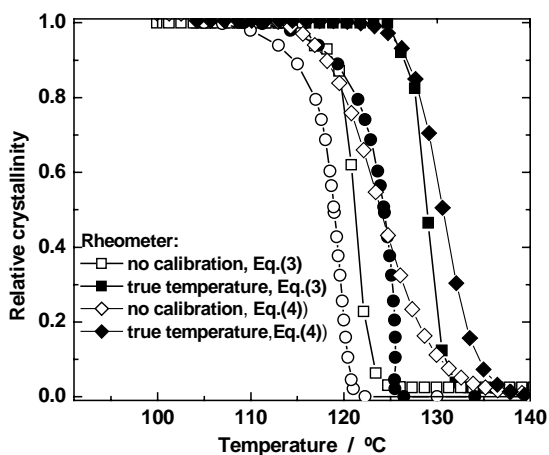


Fig. 9. Non-isothermal crystallization at  $-2^{\circ}\text{C}/\text{min}$ . DSC results without temperature correction ( $\square$ ) and after the true sample temperature evaluation ( $\blacksquare$ ). The rheometer results for the same cooling rate and for the oscillation frequency of 10 Hz are indicated by ( $\square$ ) and ( $\diamond$ ) for the results without calibration, with  $X(T)$  evaluated from Eqs. (3) and (4), respectively. The corresponding corrected temperatures are indicated by ( $\blacksquare$ ) and ( $\blacklozenge$ ).

and (4), which may seem important for the data of Fig. 5, vanishes when the true sample temperature is evaluated. Then, for isothermal crystallization experiments, the use of Eqs. (3) or (4) is irrelevant for evaluating from the rheometer data the degree of conversion to the solid phase.

### 3.3. True sample temperature in nonisothermal scans

The procedure presented in the introduction for the calibration on cooling and the true sample temperature evaluation was also applied to nonisothermal crystallization results obtained with a DSC and a rheometer for a controlled cooling rate of  $-2^{\circ}\text{C}/\text{min}$ . Fig. 9 shows the results obtained with both devices, without calibration, open symbols, and after the temperature corrections according to the procedures described in the introduction of this work, full symbols. The crystallization kinetics starts earlier for the rheometer experiments, in agreement with results obtained previously. This figure also shows the effect of using the Eqs. (3) or (4) for evaluating from the rheometer data the degree of conversion to the solid phase, before and after the temperature corrections.

For testing the accuracy of the procedure used in the data correction of Fig. 9, the predicted average true sample temperature was compared with the measured sample temperature, in real time, with the external thermocouple. The result is in Fig. 10 and the inset shows, with more detail, both results in crystallization temperature range for the particular oscillation frequency of 10 Hz and cooling rate of  $-2^{\circ}\text{C}/\text{min}$ . It must be noted again that the temperature error for the measurements with the thermocouple is  $\pm 0.5^{\circ}\text{C}$  and that the evaluated temperature error for the rheometer temperature sensor is  $\pm 0.6^{\circ}\text{C}$ . The results obtained show that,

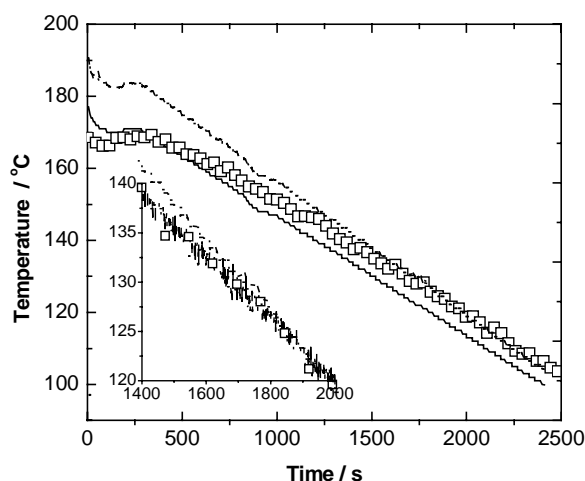


Fig. 10. Variation of the rheometer program temperature (full line), the measured sample temperature ( $\square$ ) and the corrected temperature evaluated from Eq. (1) for the cooling calibration and Eq. (2) for the true sample temperature evaluation, with  $X(T)$  of the last equation evaluated from Eq. (3) (dotted line) and Eq. (4) (dashed line). Oscillation frequency 10 Hz, cooling rate  $-2^{\circ}\text{C}/\text{min}$ , gap size 0.72 mm. The inset shows the variation of those temperatures in the temperature range of the nonisothermal crystallization experiments.

also for nonisothermal experiments, and after the true sample temperature evaluation, both Eqs. (3) and (4), could be used for evaluating from the rheometer data the degree of conversion to the solid phase. This is not a justification in favour of none of the above two equations but the above results clearly support the validity of the procedures used for calibrating the rheometer and for evaluating the average true sample temperature.

## 4. Conclusion

We have addressed in this work the temperature calibration that is of major relevancy for obtaining reliable experimental data in an experimental device where the recorded temperature is a key variable. The temperature calibrations were performed for heating, cooling and isothermal experiments, with the same metal standards used for calibrating other thermal analysis devices. The procedure for evaluating the isothermal correction was discussed, together with the surprising behaviour found for it, with the device used in this work, that is, its dependence on the approach to the nominal isothermal temperature. This behaviour was validated through measurements performed with an additional thermocouple, and also by comparing the data obtained with the rheometer and the DSC for similar crystallization conditions. The results obtained with the rheometer for samples with different thickness were analysed and the average true sample temperature estimated, leading to a good agreement, within the experimental measurement errors, between the corrected results. The procedure for performing nonisothermal crystallization studies with a

parallel plate rheometer was also described, and a method for calibrating the rheometer on cooling was presented and validated. It was also shown that the two different equations used for evaluating the degree of conversion to the solid phase yield, after the true sample temperature evaluation, similar results for isothermal and nonisothermal experiments.

### Acknowledgements

The authors acknowledge Dra. Luzia Filipe, from Borialis, Portugal, for supplying the material used in this work. This work was carried out under financial support of the European Community fund FEDER, through the project POCTI/33061/CTM/2000 approved by the Portuguese Foundation of Science and Technology (FCT), that is also acknowledged by the grant BPD/5517/2001 assigned to W. Zhang. FCT is also acknowledged for the grant BSAS/3902/2002 assigned to J.A. Martins.

### References

- [1] J.Y. Yoon, H.S. Myung, B.C. Kim, S.S. Im, *Polymer* 41 (2000) 4933–4942.
- [2] H.S. Myung, W.J. Yoon, E.S. Yoo, B.C. Kim, S.S. Im, *J. Appl. Polym. Sci.* 80 (14) (2001) 2640–2646.
- [3] E. Koscher, R. Fulchiron, *Polymer* 43 (2002) 6931–6942.
- [4] N.V. Pogodina, H.H. Winter, *Macromolecules* 31 (1998) 8164–8172.
- [5] S. Acierno, N. Grizzuti, H.H. Winter, *Macromolecules* 35 (2002) 5043–5048.
- [6] J.A. Martins, J.J.C. Cruz Pinto, *Thermochim. Acta* 332 (1999) 179–188.
- [7] H. Janeschitz-Kriegl, H. Wippel, Ch. Paulik, G. Eder, *Colloid Polym. Sci.* 271 (1993) 1107–1115.
- [8] J.A. Martins, J.J.C. Cruz Pinto, *Polymer* 41 (2000) 6875–6884.
- [9] K. Boutahar, C. Carrot, J. Guillet, *Macromolecules* 31 (1998) 1921–1929.
- [10] Y.P. Khanna, *Macromolecules* 26 (1993) 3639–3643.
- [11] I. Alig, S. Tadjakhsch, G. Floudas, C. Tsitsilianis, *Macromolecules* 31 (1998) 6917–6925.
- [12] F. Ding, A.J. Giacomin, R.B. Bird, C.B. Kweon, *J. Non-Newtonian Fluid Mech.* 86 (1999) 359–374.
- [13] J.M. Shultz, *Polymer Crystallization*, Oxford University Press, Oxford, UK, 2001.